

# Quantitative Treatment of Photochemical Effects on the Ultraviolet Resonance Raman Spectroscopic Intensities—Application to Enzymatic Cofactors Containing Dihyronicotinamide and Their Photochemically Induced Transients

Krzysztof Bajdor, Yoshifumi Nishimura, and Warner L. Peticolas\*

Contribution from the Department of Chemistry, University of Oregon, Eugene, Oregon 97403.  
Received September 18, 1986

**Abstract:** Theoretical equations for calculating the dependence of the Ultraviolet Resonance Raman (UVR) intensities of a photochemically labile molecule and its photochemically labile transient by using pulsed UV laser excitation have been derived. It is shown how to use these equations to obtain numerical values of the cross sections and quantum yields for photochemical events which are in competition with the UVR effect. UVR spectra are presented of the enzymatic cofactor nicotinamide adenine dinucleotide in its oxidized ( $\text{NAD}^+$ ) and reduced forms ( $\text{NADH}$ ) as well as the dihyronicotinamide mononucleotide (NMNH). A series of laser lines in the range of 200–355 nm from a frequency modified YAG laser were used to obtain the UVR spectra. The Raman spectra of these molecules are considerably changed by changing the wavelength of the exciting light. Our earlier observation that UVR spectra of  $\text{NADH}$  are dominated by the nicotinamide moiety at wavelengths at 330 nm or longer and by the adenine moiety at wavelengths at 300 nm or below has been confirmed. The Raman spectra of  $\text{NADH}$  and NMNH taken with the pulsed YAG laser line at 355 nm which is in resonance with their lowest allowed absorption band show an intensity dependent Raman band which is assigned to the molecular ion-radical formed by a photochemical event induced by the 355-nm pulse. The power dependence of the Raman spectra has been analyzed in detail, and the cross sections and quantum yields have been experimentally obtained. The power dependence of the growth and decay of the transient shows that the photochemically induced transient is produced by a monophotonic process and that the transient itself is highly photolabile with a cross section more than half that for the photodecomposition of the NMNH or the nicotinamide portion of  $\text{NADH}$ .

Nicotinamide adenine dinucleotide ( $\text{NAD}^+$ ) and its reduced form ( $\text{NADH}$ ) are naturally occurring enzyme cofactors which participate in various oxidation-reduction cycles. They are widely used by the dehydrogenases which incorporate these cofactors. As is well known,  $\text{NADH}$  has two chromophores that absorb strongly in the UV. These are the adenine and the dihyronicotinamide chromophores. The former has two broad absorption maxima which occur at about 260 and 210 nm while the latter has a strong absorption at about 335 nm and a second near 200 nm. A number of years ago it was shown that it is possible to distinguish between these two chromophores by using UV resonance Raman spectroscopy with exciting lines at 273 and 330 nm.<sup>1,2</sup> Raman spectra taken with wavelengths longer than 351 nm have poor signal-to-noise because of intense fluorescence of the nicotinamide moiety.<sup>1,2</sup> Recently the availability of laser lines in the range 200–355 nm from the frequency modified YAG laser<sup>3-7</sup> has permitted the UVR study of a number of aromatic nucleotide ring systems of biological interest.<sup>3-7</sup> In view of these recent developments, it seems worthwhile to continue our study of the UVR spectra of these dihyronicotinamides. This may be important since recently two laboratories have shown that a transient chemical species may be photochemically induced in dihyronicotinamides by the use of the YAG laser line at 355 nm.<sup>8,9</sup> Thus it would be of interest to see if the UVR spectra

of this photochemically induced intermediate could be observed, particularly since the study of Johnson et al.<sup>10</sup> shows clearly that under certain conditions one can observe the UVR spectra of photochemically induced transient species in certain aromatic amino acid residues and their analogues. In this paper we report the UVR spectra of the reduced and nonreduced nicotinamides at a variety of UV exciting wavelengths. Also reported is a Raman study of the transient intermediate formed from irradiation of the reduced forms at 355 nm. The equations developed by Johnson et al.<sup>10</sup> for the quantitative evaluation of photolabile molecules have been revised and extended to allow for changes in the laser pulse duration and for photochemical degradation of the photochemically produced transient. For the first time actual numerical values are obtained for photochemical cross sections and quantum yields from experimental measurement of UVR intensities.

## Materials and Methods

The Raman spectroscopic detection system used in this set of experiments is essentially that developed in this laboratory for UV laser Raman spectroscopy with pulsed lasers almost 10 years ago.<sup>11-13</sup> The recent commercial availability of the YAG laser with its frequency doubling capability and techniques for using anti-Stokes stimulated Raman scattering from hydrogen allows the extension of the pulsed UVR technique from exciting lines of about 265 nm which was the lower limit 10 years ago<sup>11-13</sup> to 200 nm or below.<sup>3-7</sup> Most of the UVR spectra which were taken with exciting light in the range 200–266 nm were taken with a solar blind phototube—a technique recently developed by Ziegler and Hudson.<sup>14</sup> However, the spectra taken at longer wavelengths including the studies made at 355 nm used the same phototubes described in our earlier UVR spectroscopic investigations.<sup>11-13</sup>

(1) Rodgers, E. G.; Peticolas, W. L. *J. Raman Spectrosc.* **1976**, *9*, 372-375.

(2) Bowman, W. D.; Spiro, T. G. *J. Raman Spectrosc.* **1976**, *9*, 369-371.

(3) Ziegler, L. D.; Strommen, D. P.; Hudson, B. S.; Peticolas, W. L. *Raman Spectroscopy, Linear and Non Linear, Proceedings of the Eighth International Conference on Raman Spectroscopy*; Lascombe, J., Huang, P. V., Eds.; John Wiley & Sons: New York, 1982; pp 337-338.

(4) Ziegler, L. D.; Strommen, D. P.; Hudson, B. S.; Peticolas, W. L. *Biopolymers* **1984**, *23*, 2067-2081.

(5) Dudik, J. M.; Johnson, C. R.; Asher, S. A. *J. Phys. Chem.* **1985**, *89*, 3805.

(6) Kubasek, W. L.; Hudson, B.; Peticolas, W. L. *Proc. Natl. Acad. Sci. U.S.A.* **1985**, *82*, 2369-2373.

(7) Fodor, S.; Rava, R. P.; Hays, T. H.; Spiro, T. G. *J. Am. Chem. Soc.* **1985**, *107*, 1520-1528.

(8) Boldridge, D. W.; Morton, T. H.; Scott, G. W. *Chem. Phys. Lett.* **1984**, *108*, 461-468.

(9) Czochralska, B.; Lindqvist, L. *Chem. Phys. Lett.* **1983**, *101*, 297-304.

(10) Johnson, C. R.; Ludwig, M.; Asher, S. A. *J. Am. Chem. Soc.* **1986**, *108*, 905-912.

(11) Blazej, D. C.; Peticolas, W. L. *Proc. Natl. Acad. Sci. U.S.A.* **1977**, *74*, 2639-2643.

(12) Chinsky, L.; Turpin, P. Y.; Duquesne, M.; Brahm, J. *Biopolymers* **1978**, *17*, 1347-1359.

(13) Blazej, D. C.; Peticolas, W. L. *J. Chem. Phys.* **1980**, *72*, 3134-3142.

(14) Ziegler, L. D.; Hudson, B. *J. Chem. Phys.* **1981**, *74*, 982-992.

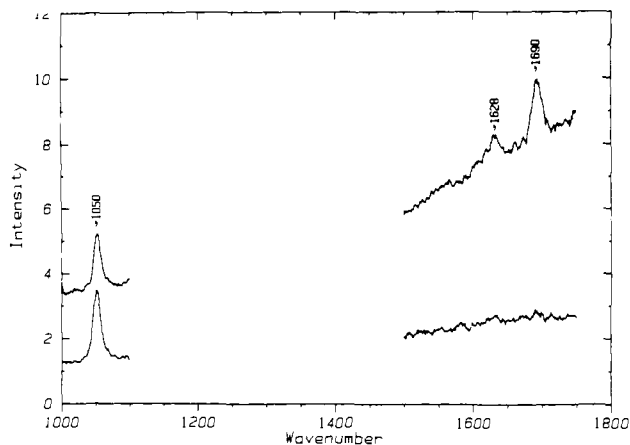


**Figure 1.** A portion of two UVRR spectra of an aqueous solution of reduced nicotinamide mononucleotide (NMNH) containing the nitrate ion as an internal standard. This spectrum was taken with 355-nm excitation, and the solution is recirculated through a flowing jet stream by using a peristaltic pump. The top spectrum is after 30 min of multiscanning. After an hour of multiscanning, the nitrate band at  $1050\text{ cm}^{-1}$  remains constant in intensity, but the bands at  $1690$  and  $1628\text{ cm}^{-1}$  due to the NMNH and its photoinduced transient, respectively, become too weak to measure, bottom spectrum.

The sampling technique used in these experiments is rather different from those employed in the previous UVRR investigations.<sup>3-7,10-13</sup> In the past it has been common practice with UVRR spectroscopy to continuously recirculate the solution containing the sample in front of the laser beam. This technique has a great disadvantage because photochemistry almost always occurs in the YAG UV pulse so that increasing amounts of photochemically degraded sample may build up within the sample solution. This can lead to very serious quantitative errors as the concentration of the sample continuously decreases. For example, Figure 1 shows two Raman spectra of an aqueous solution of reduced nicotinamide mononucleotide containing the nitrate ion as an internal standard taken at 355-nm excitation. These spectra are the results of a computer scan of the nitrate region at  $1050\text{ cm}^{-1}$  followed by a scan over the bands at  $1690$  and  $1628\text{ cm}^{-1}$  which are due to NMNH and its photoproduct, respectively. These spectra were taken by using a recirculating flowing sample which is pumped from a small flask to a jet stream which passes in front of the pulsing laser beam. The top spectrum was taken initially, and it is the results of 10 scans. The second or bottom spectrum was taken after 2 h of scanning. The nitrate peak is still visible, but the other peaks are too weak to be seen. Sometimes with use of this technique it was found that evaporation caused the solute concentrations to increase. It is obvious that any data taken in this way—which is the most common way<sup>3-7,10-14</sup>—cannot always be used reliably to obtain quantitative data on the intensities of the UVRR bands. Consequently we have developed a way which we have called the "slow-flow" method.

In the slow-flow method a glass or quartz capillary is used. When a glass capillary is used, a small hole is made in the side of the capillary with a file in order to let the focused UV laser light to impinge directly on the flowing sample. The solution flows once through the capillary and is then discarded. Because of surface tension effects, the aqueous solution does not flow out of the hole in the side of the capillary but continues its passage down the capillary and out the end. When a quartz capillary is used as it was in most of the experiments reported in this paper, the laser is not focused to such a small spot size—only to a diameter of about a third of a millimeter so that the capillary is not damaged in the laser beam. The sample flow rate through the capillary is much slower than the usual jet stream customary in these type of measurement,<sup>3-7,10-12</sup> but the flow rate is fast enough to allow the laser pulse to strike a completely new portion of sample. Since the pulses come 10 times per s and they are focused to  $0.3\text{ mm}$ , this means that the linear flow rate in the capillary must exceed  $3\text{ mm/s}$  which it did in our experiments. By using this technique we have determined the numerical values of the cross sections and quantum yields for the formation and photodegradation of the photoinduced transients.

#### Raman Spectroscopic Results on Reduced Nicotinamides

The cofactor nicotinamide adenine ( $\text{NAD}^+$ ) and its reduced form NADH contain two different chromophoric moieties, nicotinamide and adenine, with various absorption bands in the range  $200\text{--}350\text{ nm}$ . The UVRR spectroscopy of the adenine moiety has been studied in detail by using the  $200\text{--}400\text{-nm}$  YAG laser system by

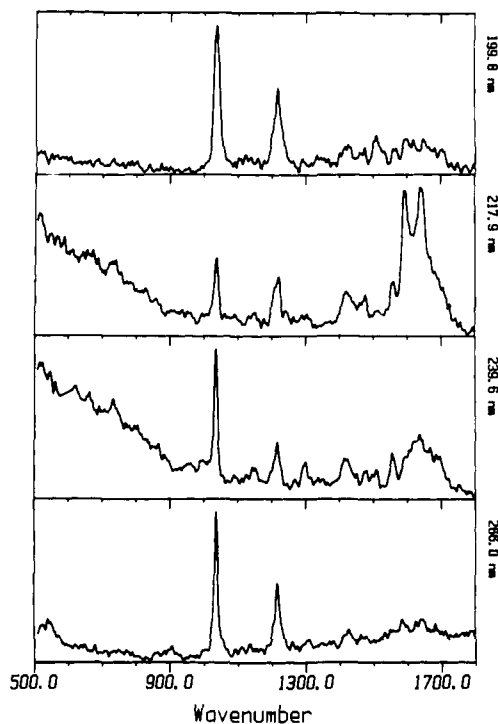


**Figure 2.** The UVRR spectra of 1-methylnicotinamide taken with exciting lines at 199.8, 217.9, 239.6, and 266 nm.

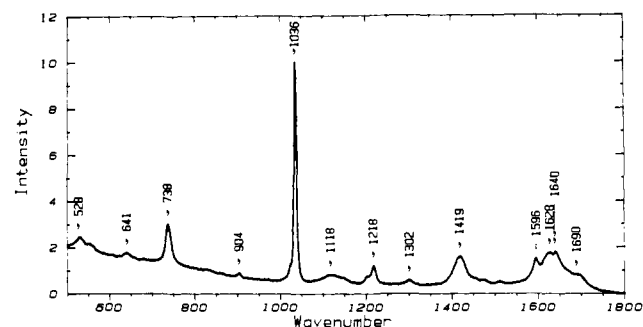


**Figure 3.** The classical Raman spectrum of 1-methylnicotinamide taken with 514.5-nm light to help with the assignment of the UVRR spectra shown in Figure 2.

several laboratories,<sup>3,4,6,7</sup> but to date no one had studied the UVRR spectra of the nicotinamide moiety over this frequency range. Figure 2 shows the UVRR spectra of 1-methylnicotinamide taken with four lines from the frequency modified YAG laser: 199.8, 217.9, 239.6, and 266.0 nm. For comparison and to help in assignments, Figure 3 shows the classical Raman spectrum of 1-methylnicotinamide taken at 514 nm. What is particularly remarkable about the series of UVRR spectra is that two sharp bands at  $1585$  and  $1640\text{ cm}^{-1}$  appear very strongly in the UVRR spectrum taken at  $218\text{ nm}$  but are very weak in the spectrum at  $240\text{ nm}$  and do not appear at all in the other UVRR spectra. These bands probably correspond to the weak bands at the same frequency in the classical spectrum (Figure 3) except that the band at  $1640\text{ cm}^{-1}$  is a doublet in the classical spectrum. The band at  $1640\text{ cm}^{-1}$  may be due to the carbonyl (amide-I) band nicotinamide. This would seem to indicate that an UV absorption band with a fairly sharp maximum near the frequency of  $218\text{ nm}$  is present in 1-methylnicotinamide. This absorption band must involve the electrons in the carbonyl band and appears to be hidden in the overall broad absorption of the molecule. The sharp, narrow band at  $1036\text{ cm}^{-1}$  is assigned to ring breathing mode (similar to the  $992\text{-cm}^{-1}$  band of benzene).

Figure 4 shows the UVRR spectra of NAD taken at the same set of frequencies as in Figure 2. These spectra are for the most part dominated by the adenine moiety as was previously reported.<sup>1</sup> This domination of the UVRR spectrum by the adenine Raman

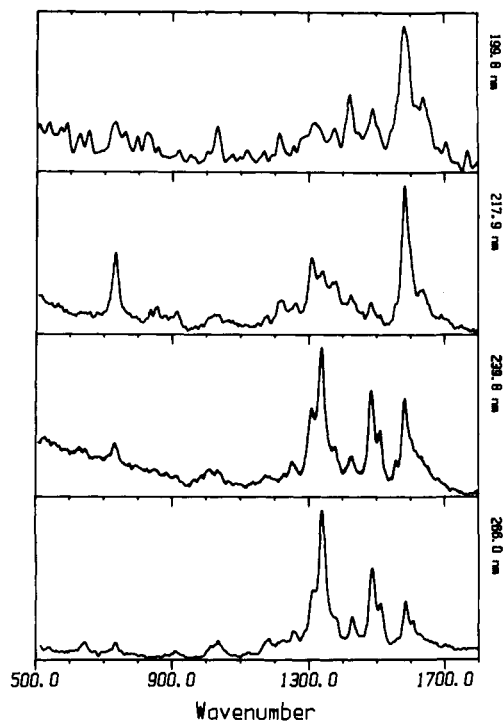


Figure 4. The UVRR spectra of NAD<sup>+</sup> taken with the same set of excitation frequencies as shown in Figure 2. These spectra are for the most part dominated by the adenine moiety.

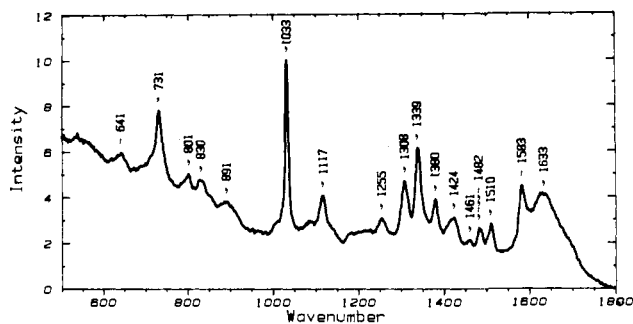


Figure 5. The classical Raman of NAD<sup>+</sup> taken with 514.5-nm exciting light to help with the assignments of the UVRR spectra shown in Figure 4.

bands appears to be due to the stronger absorption of adenine in this region. This domination by the adenine bands does not occur in the classical Raman spectrum of NAD shown in Figure 5. Here one can see bands due to both adenine and nicotinamide.<sup>1,2</sup> In the reduced form, the adenine, NADH, also dominates most of the UVRR spectra in the 200–300-nm frequency region as shown in Figure 6 so that the UVRR spectra of NAD and NADH are almost identical with adenosine as the wavelength is scanned from 200–266 nm. However, there is one important exception to this observation. In the UVRR spectrum of NADH taken at 200 nm a strong new band appears at 1690 cm<sup>-1</sup>. This is most likely the band at 1690 cm<sup>-1</sup> shown in Figure 7 in the classical Raman spectrum of NADH. Although this band had been assigned earlier to the amide I or carbonyl vibration,<sup>2,15,16</sup> recent work in this laboratory has led to the suggestion that this assignment may not be entirely correct.<sup>1</sup> The amide I vibration is usually broad, sensitive to the environment, and involves a contribution due to coupling to the C–NH group. It generally shifts 5–20 cm<sup>-1</sup> upon deuterium exchange because of the heavier mass of the –ND group. Furthermore, all carbonyl groups decrease in frequency as the dielectric constant of the solvent is increased due to an

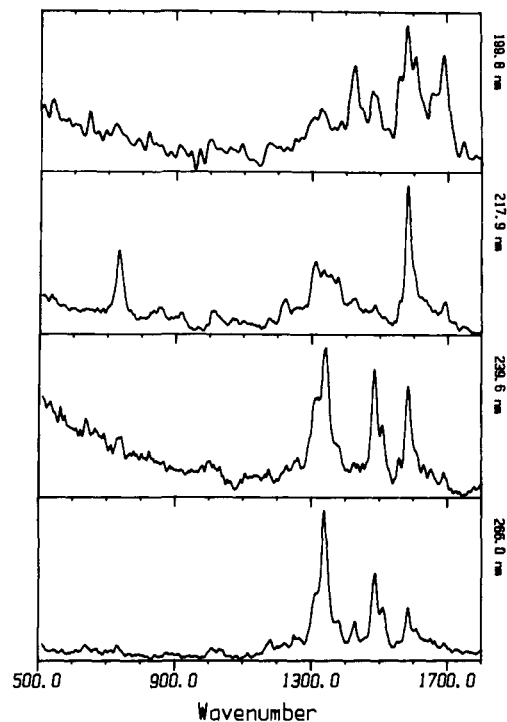


Figure 6. The UVRR spectra of NADH taken with the same set of excitation frequencies as shown in Figures 2 and 4.

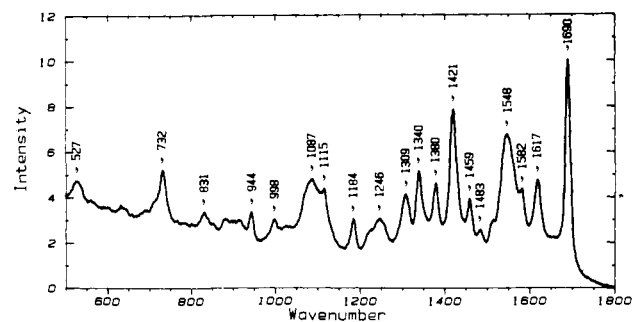


Figure 7. The classical Raman spectrum of NADH taken with 514.5-nm excitation to help with the assignments of the UVRR spectra shown in Figure 6.

increased polarization of the C=O linkage with increased charge separation and decreasing bond order. However the 1690-cm<sup>-1</sup> band of NADH shows none of these characteristics. It was pointed out<sup>1</sup> that 1,4-cyclohexadiene has a band at 1680 cm<sup>-1</sup> due to the C=C symmetric stretching motion of the two double bonds and that this motion may also be involved in the 1690-cm<sup>-1</sup> band found in the reduced dihydronicotinamides. We see in Figure 6 that this band in NADH comes on strong resonance at 200 nm. Thus it seems likely that the band at 1690 cm<sup>-1</sup> is a mixture of C=C double bond stretch and C=O amide vibration coupled in such a way that the coupling to the vibrations of the NH<sub>2</sub> group is reduced.

In order to further test the idea that this prominent band at 1690 cm<sup>-1</sup> includes an important contribution from the C=C double bond stretching motion, we have performed two experiments. First, we have taken the spectra of the reduced  $\beta$ -nicotinamide mononucleotide (NMNH) over the same frequency range as shown in Figure 2. In view of the fact that the absorption spectrum of NMNH shows no maxima between 350 and 200 nm we expect very weak or nonexistent UVRR spectra except for the 200 nm excited UVRR spectrum. Second, in view of the assignment of the 1690-cm<sup>-1</sup> band in NADH to a complex mode which involves the C=C double bond stretching motion of the reduced nicotinamide ring, we would expect the reduced form of the nicotinamide mononucleotide to show the same resonance enhancement of this 1690-cm<sup>-1</sup> band with 200-nm excitation.

(15) Patrick II, D. M.; Wilson, J. E.; Leroy, G. E. *Biochemistry* **1974**, *13*, 2813–821.

(16) Forrest, G. *J. Phys. Chem.* **1976**, *80*, 1127–1128.

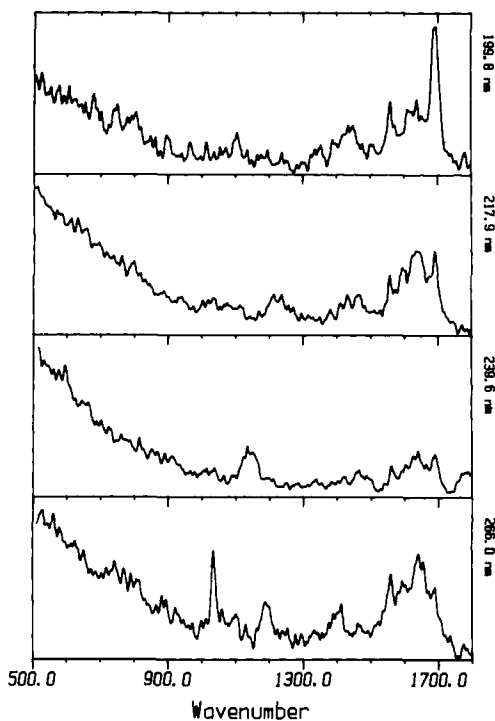


Figure 8. The UVR spectra of reduced nicotinamide mononucleotide, NMNH with the same set of excitation frequencies and taken under the same set of conditions as the UVR spectra shown in Figures 2, 4, and 6.

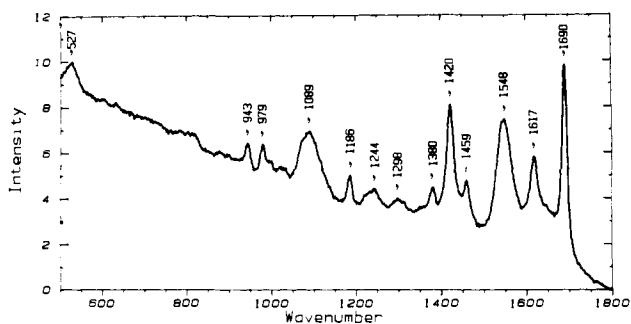


Figure 9. The classical Raman spectrum of NMNH taken with 514.5-nm excitation to help with the assignments of the UVR spectra shown in Figure 8.

Figure 8 shows the spectra, and our expectations are readily borne out. The spectra at 218, 240, and 266 nm are weak and noisy, but they show identifiable bands in the region 1500–1700  $\text{cm}^{-1}$ . These are probably due to the same vibrations as those shown in the same frequency region in the classical Raman spectrum of reduced nicotinamide mononucleotide shown in Figure 9. On the other hand the spectrum taken with 200-nm light shows the band at 1690  $\text{cm}^{-1}$  as expected. Thus the 1690- $\text{cm}^{-1}$  band in NADH plainly comes from the reduced nicotinamide moiety, and this band does not show strong resonance enhancement with exciting light in the region 300–218 nm. Since this 1690- $\text{cm}^{-1}$  band does show strong resonance enhancement at 200-nm incident light as well as the previously observed resonance enhancement at 330 nm,<sup>1,2</sup> one may conclude that both the 340- and the 200-nm absorption bands of the reduced form of nicotinamide involve a displacement of the C=C bond in the excited state in addition to a possible contribution from the C=O band.

The second experiment we performed in order to give further evidence that the 1690- $\text{cm}^{-1}$  band of the reduced nicotinamide moiety involved the double bond stretching vibration of the C=C double bonds was to look at the UVR spectra of 1,4-cyclohexadiene. This molecule shows an absorption just below 200 nm with a pronounced shoulder at 210–215 nm. If we assume that these observed absorption bands in the region 200–210 nm in both compounds come from the similar  $\pi-\pi^*$  transitions, then the band

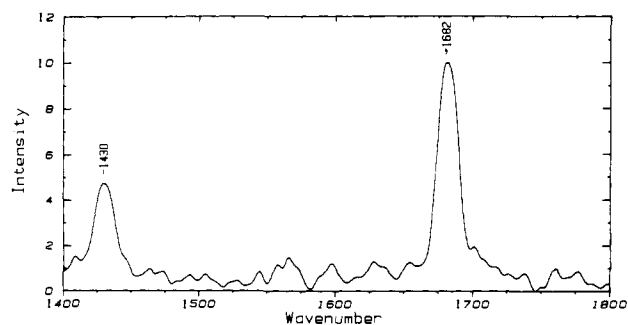


Figure 10. The UVR spectrum of cyclohexadiene taken at 218 nm.

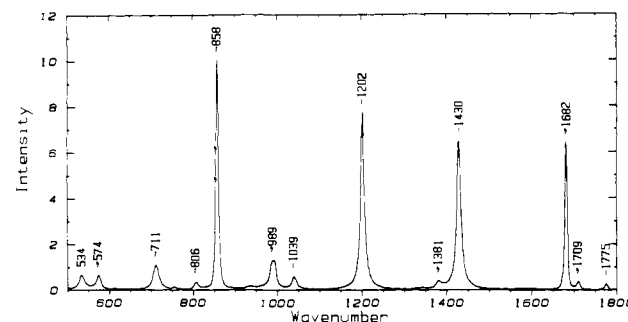


Figure 11. The classical Raman spectrum of 1,4-cyclohexadiene taken at 514.5 nm.

at 1680  $\text{cm}^{-1}$  which appears in the classical Raman spectrum of 1,4-cyclohexadiene should show resonance in the 200–210 region. Figure 10 shows the UVR spectrum of cyclohexadiene taken at 218 nm, and the resonance enhancement of the 1680- $\text{cm}^{-1}$  line is plainly evident. Thus it may be concluded that the shoulder at 210–215 nm is an absorption band from an electronic state which involves a displacement of the C=C double bonds in the excited state. Interestingly, we were not able to obtain a UVR spectrum of the 1,4-cyclohexadiene with the 200-nm line of the frequency modified YAG laser. The reason for this is not entirely clear but seems to arise from the fact that the resonance enhancement arises from the absorption band which is a shoulder at 210–215 nm and not from the band with a maximum below 200 nm. This latter band does not appear to give strong resonance enhancement at 200-nm excitation. Figure 11 shows the classical Raman spectrum of 1,4-cyclohexadiene taken at 514 nm. It is of interest that only the 1682- and the 1430- $\text{cm}^{-1}$  bands are present in both the classical and UVR spectrum.

Figure 12 shows the Raman spectrum of NADH in the region 1550–1750  $\text{cm}^{-1}$  taken with 355-nm excitation at several different power settings for the YAG laser. This figure shows the growth of the band at 1628  $\text{cm}^{-1}$  with increasing power of the laser pulses. We tentatively assign this band to the C=C stretching of the cation radical formed from the reduced NMNH by the 355-nm laser pulses.<sup>8,9</sup> The lower frequency may be due to the loss of an electron from the aromatic region causing a reduced bond order in the double bond. We now describe a quantitative theoretical technique for determining the cross sections for the photodecomposition of a photolabile molecule.

**Theory of the Laser Intensity Dependence of the UVR Scattering from Photolabile Molecules and Their Photochemically Produced Transients.** Although the theory of the laser intensity dependence of the Raman scattering intensity from photolabile molecules and their photochemically produced transients was originally carried out in the pioneering paper of Johnson et al.,<sup>10</sup> these authors made no attempt to show a quantitative application of their theory. Although the equation they developed for the photolabile precursor will give a reasonable fit to their observed experimental points, their theory for the photochemically induced transient gives a result which is in disagreement with the experimental data which they presented in their figures. Their theory is also in disagreement with the data presented here on the photoinduced transients of reduced nicotinamides. Indeed al-

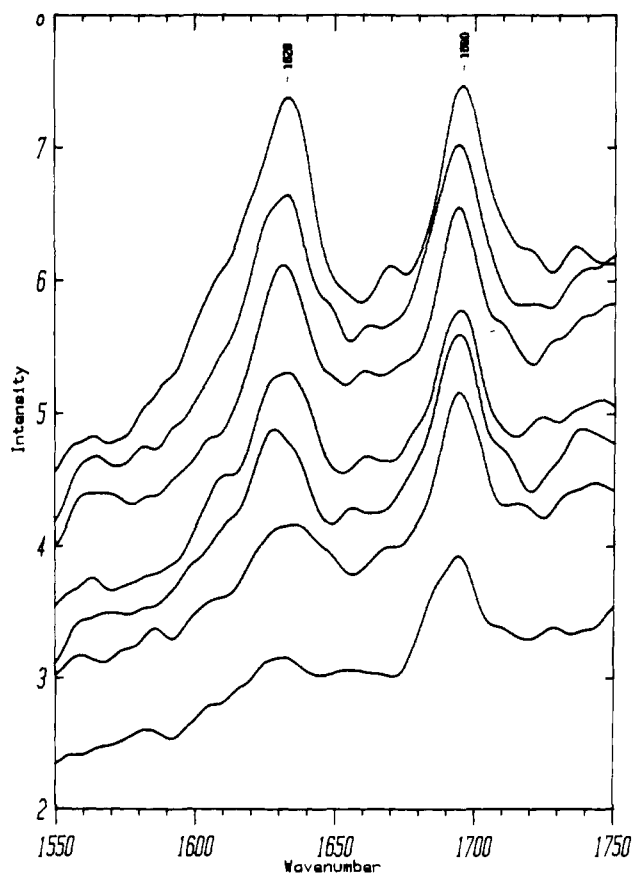


Figure 12. The Raman spectrum of NADH taken with 355-nm laser light by using several different peak laser intensities showing the growth of the band at  $1628\text{ cm}^{-1}$  due to the photochemically induced transient.

though their equations predict a rather drastic difference in the laser intensity dependence of the Raman scattering intensity from the photolabile precursor and the transient species, their experimental data show a remarkable similarity in the laser intensity dependence of the two species. In the following we will rederive the laser intensity dependence of the resonance Raman intensity for both the precursor and the transient species and show how these equations can be used to calculate curves which agree very closely to experimental data. From this quantitative agreement important experimental parameters may be obtained. This quantitative agreement between calculation and experimental measurements on these photolabile systems has never been attempted before. It gives us a much better understanding of the competition between photochemistry and UVRR scattering from organic molecules—almost all of which must be considered photolabile under the conditions of the resonance Raman effect from pulsed lasers with peak powers in the MW range. It must be noted that the approach used here is also approximate since it does not use the population of the excited state of the precursor. A more complete theory is given in the Appendix. It appears that for the few quantitative experimental data currently available, the approach used in this section appears to be adequate.

Consider the behavior of a photochemically induced reaction under the influence of a square wave pulse of light of intensity  $I_0$  photons/cm<sup>2</sup>s during the pulse which has a pulse width  $\tau \approx 6$  ns. This is a good approximation to the pulse shape of the Quanta-Ray YAG laser according to their instruction booklet.<sup>17</sup> If  $P$  is the concentration of the molecules initially present, the precursor, then the rate of depletion of precursor is given by

$$dP/dt = -\sigma_A I(t)P$$

where  $\sigma_A$  is the cross section for the photochemical decomposition

of  $P$ , and  $I(t)$  is the intensity of the laser as a function of time,  $t$ . Johnson et al.<sup>10</sup> integrated this equation over  $t = 0$  to  $\infty$ ; we will integrate from  $t = 0$  to  $\tau$ , the pulse width of the YAG laser. In this way we can take account of the effect of different pulse widths. However, for  $t < \tau$  the time dependence of the concentration dependence of  $P$  is given by

$$P(t) = P_0 \exp(-\sigma_A I_0 t)$$

For times,  $t > \tau$ , the concentration of  $P$  remains constant

$$P(t) = P_0 \exp(-\sigma_A I_0 \tau); \quad t > \tau$$

These integrated equations for the concentration of  $P$  as a function of time are only valid if, as we have emphasized in the experimental section, each pulse of the laser impinges upon a fresh sample. It would be difficult, perhaps impossible, to develop a theory for the time dependence of  $P$  which would be valid for samples which are recirculated through the laser beam as is customary in much recent work.<sup>3-7,10-13</sup>

Let  $I_P$  be the Raman photons/cm<sup>3</sup> produced from the precursor molecules during the laser pulse. The scattered resonance Raman band intensities are proportional to the total number of these Raman photons created during one pulse which is given by

$$I_P = \int \sigma_p I(t) P(t) dt, \quad \text{or}$$

$$I_P = (\sigma_p P_0 / \sigma_A) [1 - \exp(-\sigma_A I_0 \tau)] \quad (1)$$

where  $\sigma_p$  is the cross section for Raman scattering from the initial molecule present for the precursor,  $P$ . Notice how the pulse width,  $\tau$ , enters into our formulation of the theory in a natural way. In the limit when the cross section for the photochemical decomposition of the precursor,  $\sigma_A$ , goes to zero we have

$$I_P = \sigma_p I_0 \tau P_0$$

Thus when there is no photochemistry competing with the UVRR scattering, the measured Raman intensity is linearly proportional to the pulse length, the incident intensity, the molecular concentration, and the scattering cross section. We will emphasize the necessity of considering the limits of these equations as we go along. Plots of  $I_P$  vs. the laser intensity,  $I_0$ , using eq 1 with reasonable values of the parameters, shows curves similar to those which have been measured by Johnson et al.<sup>10</sup> and reported by us below for the intensity of a UVRR band of an organic molecule taken as a function of the intensity of the incident YAG laser pulse for photolabile molecules.

In order to obtain the dependence of the Raman intensity of the photoinduced transient on the intensity of the laser pulse, it is necessary to assume that the only photodecomposition product of the precursor is the formation of the transient intermediate. Measurements of the time dependence of this photochemical process for reduced nicotinamides by Bolderidge et al.<sup>8</sup> show that the lifetime of the transient produced by the photochemical decomposition of reduced nicotinamides is long compared to the YAG laser pulse width so we do not have to worry about depletion of the transient by spontaneous decay. It is necessary to realize that the transient intermediate itself is also photolabile and that it will undergo photodecomposition as the laser power is increased and that this photodecomposition must be accounted for in the theory if quantitative agreement is to be obtained. It is the failure to include the photodecomposition of the photoproduct transient intermediate which leads to equations which are not in agreement with experiment by Johnson et al.<sup>10</sup> However, we will start by assuming that the transient intermediate is not photolabile and show how the resulting equation does not agree with either the experiments of Johnson et al.<sup>10</sup> or with our experiments on the reduced nicotinamides. Then we will show how to incorporate the photodecomposition of the transient intermediate in a simple way and obtain equations which will quantitatively predict the laser power dependence of the photoproduct transient.

If the only photodecomposition product of the photolabile precursor,  $P$ , is the transient,  $T$ , and this transient is not photolabile, then the concentration of  $T(t)$  as a function of time is given by

(17) Quanta Ray Instruction Manual for YAG laser, obtainable from Quanta Ray division of Spectra Physics, Mountain View, CA.

$$T(t) = P_0 - P(t) = P_0[1 - \exp(-\sigma_A I_0 t)]$$

The total number of UVRR photons produced from the transient during a laser pulse is given by

$$I_T = \int \sigma_T I(t) T(t) dt, \quad \text{or}$$

$$I_T = \sigma_T I_0 \tau P_0 - (\sigma_T P_0 / \sigma_A) [1 - \exp(-\sigma_A I_0 \tau)] \quad (2)$$

If we take the limit as  $\sigma_A$  goes to zero, thus suppressing the formation of the transient intermediate, we find that the Raman scattering intensity,  $I_T$ , goes to zero as it must. Except for the explicit inclusion of the pulse width, this equation is identical with that of Johnson et al.<sup>10</sup> Typical plots of the UVRR intensity of a transient intermediate as a function of laser power which are obtained from eq 2 show a continually increasing intensity in the Raman spectra of the intermediate starting with a square dependence on laser power at low intensities and a linear dependence in the limit of high intensities. The curves calculated do not resemble at all the reported experimental measurements of Johnson et al. or of our own as we will discuss below in detail. However, the initial square dependence on the laser power was noted by Johnson et al.<sup>10</sup> and can be observed in their very low intensity data.

In order to obtain curves which agree with the experiment we must take into account the fact that the photochemically induced transient itself is a photolabile organic molecule under the conditions of UVRR spectroscopy with pulsed lasers with MW peak power. At low incident pulsed laser powers the Raman bands of the transient will increase rapidly with laser power because more transient species are formed as the laser power is increased and the intensity of the Raman scattered light from a given number of transient molecules also increases. This is the origin of the initial square dependence of the Raman bands of the transient on the laser power. However, the concentration of the transient molecules must be diminished by the laser induced photochemical decomposition of the transient species. When this effect is large, the intensity of the Raman light from the transient will tend to level off as the power of the laser pulses are increased. To take care of this phenomenon, we propose a very simple correction. We start with the concentration of the transient,  $T(t)$ , which is increased by the depletion of the precursor,  $P(t)$ , and decreased by laser-induced photodecomposition which occurs with a cross section,  $\sigma_D$ . In this approximation, the time dependence of the concentration of the transient intermediate,  $T(t)$ , is obtained from the following differential equation which includes buildup of the intermediate due to photodecomposition of the precursor,  $-dP/dt$ , and photochemical induced decay,  $-\sigma_D I_0 T$

$$dT/dt = \sigma_A I_0 P_0 \exp(-\sigma_A I_0 t) - \sigma_D I_0 T$$

It is simple to show that the solution of this differential equation for  $T(t)$  is

$$T(t) = \sigma_A P_0 [\exp(-\sigma_D I_0 t) - \exp(-\sigma_A I_0 t)] / (\sigma_A - \sigma_D)$$

In the limit of  $\sigma_D$  going to zero, this equation becomes identical with that obtained above for  $T(t)$  in the absence of photochemical decomposition of the transient intermediate. Integrating this equation over the pulse width to calculate the total Raman photons/cm<sup>3</sup> per pulse coming from the transient we obtain

$$I_T = [(\sigma_T P_0) / (\sigma_A - \sigma_D)] [(\sigma_A / \sigma_D) (1 - \exp(-\sigma_D I_0 \tau)) - (1 - \exp(-\sigma_A I_0 \tau))] \quad (3)$$

If the limit of this expression is taken as  $\sigma_D$  goes to zero, eq 2 above is obtained for  $I_T$  in the absence of photodecomposition of the transient intermediate.

Plots of the calculated UVRR intensity of a photochemically produced intermediate as a function of YAG laser power for various values of the parameters obtained by using eq 3 show results typical of those reported by Johnson et al.<sup>10</sup> when the cross section for the photodecomposition of the intermediate,  $\sigma_D$ , is very close in value to the cross section for the photochemical decomposition of the precursor,  $\sigma_A$ . As will be shown below this eq 3 exactly reproduces our own experimental curves for the Raman

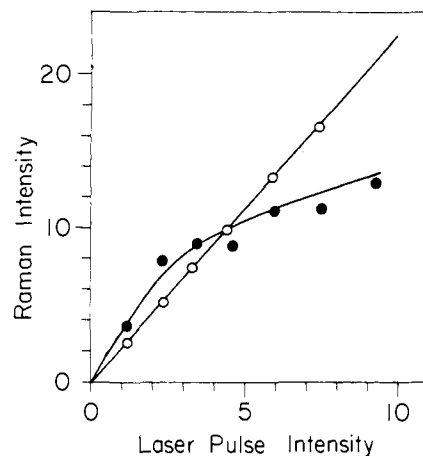


Figure 13. The intensity of the UVRR band at 1690 cm<sup>-1</sup> taken with 355-nm excitation as a function of the average power of the pulsed YAG laser in mW. To convert from average power to the laser power during the 5-ns pulse, see text. The 1690-cm<sup>-1</sup> band is a vibration of the reduced nicotinamide ring which we have assigned to the C=C bond but is usually assigned to the amide I vibration. The drawn curve is calculated by theory. The open circles show the intensity dependence of the NO<sub>2</sub><sup>-</sup> vibration.

intensity of the photoinduced transient intermediate of reduced nicotinamides as a function of laser power. In the next section we discuss the quantitative application of these equations to our experimental measurements on the photochemical product of reduced nicotinamides and show how to evaluate the various cross sections and the corresponding yields.

**Calculation of the Laser Intensity Dependence of the UVRR Scattering from Photolabile Molecules and Their Photochemical Produced Transients—Evaluation of Capture Cross Sections and Quantum Yields of Photochemical Events.** In this section we will show how it is possible to calculate the capture cross sections and quantum yields of photochemical events by using the power dependence of resonance Raman bands from a pulsed YAG laser. The lifetime,  $\tau$ , of the Quanta Ray YAG laser we used is approximately 5 ns. For each mW of average power (as measured in the laboratory) we must calculate the power which exists during the pulse. With 10 pulses a second, one calculates that a power of 20 kW is produced during the pulse. This power was focused into a circle 0.33 mm in diameter to give a light intensity during the pulse of  $2.8 \times 10^7$  joules/cm<sup>2</sup> s or for 355-nm light,  $5.0 \times 10^{25}$  photons/cm<sup>2</sup> s per mW of average laser power. This pulsed power was made to fall on a sample which was flowing rather slowly through a quartz capillary but still fast enough that each pulse falls on a fresh quantity of solution as described in Materials and Methods.

Figure 13 shows two plots of the intensity of a Raman band vs. the average intensity of the YAG laser at 355 nm. The straight line is the intensity of the Raman band at 1050 cm<sup>-1</sup> due to the nitrate ion which was used as an internal standard. This straight line behavior is typical of the behavior of the Raman spectra of nonphotolabile ions or molecules under excitation with the YAG laser. The curved plot is a plot of the intensity of the Raman band at 1690 cm<sup>-1</sup> which is due to reduced nicotinamide mononucleotide as a function of the average laser power in mW. The solid curve in Figure 13 is calculated by eq 1 by using the following values for the adjustable parameters

$$I_p = 1.6[1 - \exp(2.1 I_0)]$$

where the units of  $I_p$  are arbitrary, but the units of  $I_0$  are in mW of average power. From these experimental data we can calculate an approximate value of the cross section for the photodecomposition of reduced nicotinamide mononucleotide,  $\sigma_A \approx 0.7 \times 10^{-17}$ . The molar absorption coefficient of this molecule at 355 nm (about 5000 L/mol-cm) corresponds to an absorption cross section of about  $2.1 \times 10^{-17}$ . The ratio of these cross sections gives a quantum yield of 30–40% for the conversion of the NMH to the anion radical transient. This is in reasonable agreement with the

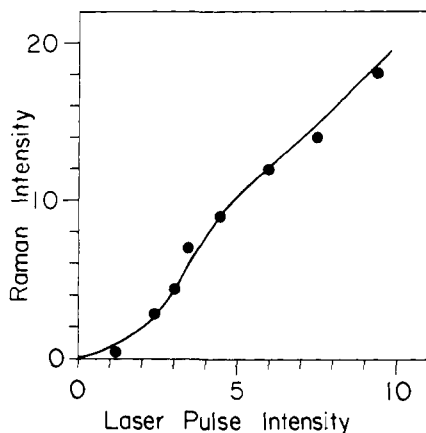


**Figure 14.** The intensity of the UVRB band at  $1628\text{ cm}^{-1}$  taken with the 355-nm excitation as a function of the average power of the pulsed YAG laser in mW. This band is assigned to the anion radical which is formed by the photodecomposition of the reduced nicotinamide moiety and which itself is photolabile.

measurements of Boldridge et al.<sup>8</sup> who estimate 50% quantum yield.

To obtain the cross section for the photodecomposition of the photoinduced transient, we use eq 3 but restrict the value of  $\tau\sigma_A$  to 2.1 found by using eq 1. This assumes that all of the photodecomposition of the precursor is due to the formation of the transient. Figure 14 shows a plot of the intensity of the band at  $1628\text{ cm}^{-1}$  which is due to the photoinduced transient intermediate as a function of the average laser power in mW. The solid line is calculated from the equation

$$I_T = 8.5[(1 - \exp(-1.35I_0))(2.1/1.35) - (1 - \exp(-2.1I_0))]$$

From this measurement we estimate a cross section for the photodecomposition of the transient,  $\sigma_T \approx 1.5 \times 10^{-17}$ . It should be noted that when the cross section for the decomposition of the transient equals that for the precursor, that no measurable amount of transient is formed. The published curves for the intensity of the UVRB bands of the tyrosinate ion vs. laser power by Johnson et al.<sup>10</sup> decrease in slope very quickly as the laser power is increased showing that in the tyrosinate ion the photoproducted transient is also very photolabile so that the intensity of the UVRB band of the transient levels falls off as the power is increased.

Since the absorption cross section of the transient is not known, we cannot estimate the quantum yield, but assuming a molar absorption of  $10^4$  one obtains an estimate of the order of 20–40%. Thus in conclusion it may be stated that we have shown how to obtain experimental values of the capture cross sections for the photoinduced decomposition of a molecule being studied by UVRB spectroscopy. When a photochemical induced transient is formed, we have shown how to obtain the capture cross section for the photoinduced decay of this transient. In both cases we have shown how to obtain the quantum yield. This procedure should find use in the study of photochemically induced reactions in which both the starting material and the product are active in the UVRB effect.

**Acknowledgment.** We acknowledge the support of this research by grants from the National Science Foundation (DMB-8417199) and the National Institutes of Health (GM 15547-18). Support from the NSF–Japan–USA Cooperative program research grant INT 831-2052 is also acknowledged.

## Appendix

The theory given in the text is only approximate since the population of the excited electronic state of the precursor is omitted. Here we will give the more exact theory which includes the excited state explicitly and show the approximations which lead to the equations given above in the text. Let  $P$  be the concentration of the precursor in the ground state and  $P^*$  be the excited state concentration. In the ground state and  $P^*$  be the excited state concentration. A precursor molecule in the excited state can either decay to the ground state with relaxation time  $\tau_1$  through fluorescence and nonradiative processes or it can be converted by means of a relaxation process with a relaxation time  $\tau_2$  to transient species leading to a photochemical conversion of precursor to transient. Let  $T$  be the concentration of transient molecules in the ground state, and  $T^*$  be the concentration of excited state transient molecules. For simplicity we assume that all of the excited state transient molecules are lost to the system. These assumptions lead to the following coupled differential equations

$$dP/dt = -aP + bP^*$$

$$dP^*/dt = aP - (b + c)P^*$$

$$dT/dt = cP^* - dT$$

$a = \sigma_{Ab}I(t)$ , where  $\sigma_{Ab}$  is the absorption cross section;  $b$  and  $c$  are the reciprocal relaxation times  $1/\tau_1$  and  $1/\tau_2$ , respectively;  $d = \sigma_D I(t)$ . The general solutions for  $P$ ,  $P^*$ , and  $T$  are

$$P = P_0[(D_2 + a) \exp(D_1 t) - (D_1 + a) \exp(D_2 t)] / (D_2 - D_1)$$

$$P^* = aP_0[\exp(D_2 t) - \exp(D_1 t)] / (D_2 - D_1)$$

$$T = acP_0\{-\exp(D_1 t)\} / [(D_1 + d)(D_2 - D_1)] + \{\exp(D_2 t)\} / [(D_2 + d)(D_2 - D_1)] + \{\exp(-dt)\} / [(D_1 + d)(D_2 + d)]$$

where  $D_1$  and  $D_2$  are given by  $D_-$  and  $D_+$ , respectively

$$D_{\pm} = [-(a + b + c) \pm \{(a + b + c)^2 - 4ac\}^{1/2}] / 2$$

The relation between the more exact equations given here in the Appendix and the more approximate equations used in the text may be seen as follows. If we assume that during the pulse a steady-state concentration of  $P^*$  is obtained, then  $dP^*/dt = 0$  so that

$$P^* = \sigma_{Ab}I(t)P / (1/\tau_1 + 1/\tau_2)$$

The relation between  $\sigma_{Ab}$  and  $\sigma_A$  is given by

$$\sigma_A = \sigma_{Ab}\phi_2 \text{ where}$$

$$\phi_2 = (1/\tau_2) / (1/\tau_1 + 1/\tau_2) = 1 - \phi_1$$

Starting with the approximate equation in the text we can derive the more exact equations as follows

$$dP/dt = -\sigma_A I(t)P = -\sigma_{Ab} I(t)P(1 - \phi_1), \quad \text{or}$$

$$dP/dt = -\sigma_{Ab} I(t)P + (1/\tau_1)P^* = -aP + bP^*$$

Thus the equations developed in the body of the text must be considered only approximations which are strictly valid when the pulse is sufficiently long that a steady state is set up. However, they appear adequate to fit the experimental data which are relatively few in number. If one had many more points with high signal to noise, then one could attempt to fit these more detailed data with the more complete equations given here in the Appendix.